A three dimensional plasticity model for sands based on state concept

Saumyasuchi Das[1, a], Brendon Bradley[1,b] and Misko Cubrinovski[1,c]

[1]University of Canterbury, New Zealand

[a]saumyasuchi.das@pg.canterbury.ac.nz, [b]brendon.bradley@canterbury.ac.nz, [c]misko.cubrinovski@canterbury.ac.nz

Keywords: three-dimensional, plasticity model, sand, hypoplasticity, stress-dilatancy

Abstract. A three dimensional plasticity model for shear deformation in sand is developed based on the plane strain model of Cubrinovski and Ishihara [1]. The model uses a circular bounding surface. The model is hypoplastic in nature, rendering the principal directions of plastic strain increment different from those of the stress, and thus, allows for accumulation of plastic strain with principal stress rotation. The model uses the multi-surface based mixed hardening rule. This paper presents results from simulations under bi-directional (torsional-stress path) uniform stress cycles, as well as bi-directional stress-controlled simulation results, where two orthogonal horizontal components of a ground acceleration time series are converted to bi-directional stress history, providing a rigorous verification of the algorithm.

Introduction

The model presented herein is a three-dimensional extension of the plane-strain model originally proposed in [1]. The original model was developed to simulate liquefaction behaviour of sands, in particular, cyclic mobility. However, the plane-strain model can consider only one horizontal component of ground motion. In fact, to date, most of the studies on liquefaction are based on the concept of simple shear that replicates a single component of ground motion. With a three dimensional model, effect of two horizontal components on liquefaction behaviour can be studied. The salient features of the plane-strain model, which are also incorporated in the three-dimensional version, are: (i) the model is based on state concept [2]; (ii) the model is hypoplastic in nature; (iii) the stress-dilatancy relationship is derived from energy consideration and is strain dependent [3]; and (iv) the model uses multi-surface based mixed hardening rule so that the complex loading cycles during earthquakes can be modeled within the mathematical and physical restrictions; for example, there is no overshooting of the backbone curve that one encounters with bounding surface formulation of plastic modulus.

Plasticity formulation

The rate-independent incremental plasticity formulation is presented herein using standard tensor notations given in the Appendix; for brevity only model specific details are presented. The generalized shear stress and the generalized plastic shear strain are defined in Eq. 1 as deviatoric invariants. Such definitions are required to maintain consistency with the definition of the plastic modulus of the original plane-strain model.

$$q = \left(s_{ij}s_{ij}/2\right)^{1/2};\;\; \eta = q/p = \left(r_{ij}r_{ij}/2\right)^{1/2};\quad \lambda = \left(2d\varepsilon_{ij}^{p}d\varepsilon_{ij}^{p}\right)^{1/2};\;\; \varepsilon^{p} = \sum\lambda \tag{1}$$

The general postulations of the plasticity theory used in this model are given in Eq. 2.

$$d\epsilon_{ij}^{p} = \lambda\,\partial g/\partial\sigma_{ij};\quad \lambda = 1/H_p\left(\partial f/\partial\sigma_{ij}\right)d\sigma_{ij};\quad d\sigma_{ij} = E_{ijkl}\left(d\epsilon_{ij} - d\epsilon_{ij}^{p}\right) \tag{2}$$

Bounding surface. The model is formulated in normalized stress space where stresses are normalized with respect to effective pressure because the backbone curve in terms of η versus ε^p is strain hardening in nature. The model assumes a circular failure surface given by Eq. 3. The failure

surface is actually a bounding surface [4] because the plastic modulus becomes zero when stress state lies on it.

$$F(r_{ij}) = \sqrt{(r_{ij} - a_{ij})(r_{ij} - a_{ij})/2} - \eta_{max} = 0 \tag{3}$$

The failure surface can be considered either of J_2 type or a special case of the general type $F(J_2, J_3) = 0$ where $J_3 = 0$ that occurs when the b value is 0.5. In the majority of seismic response analysis, models are subjected to simple shear, where shear stresses develop solely due to tractions or transverse shears from bi-directional horizontal components of ground motions. Hence, even if the failure surface incorporates the effect of b value via J_3, during simulations, the failure surface reduces to the J_2 form. Eq. 3 maintains consistency of the b value with the original plane-strain model.

Inherent anisotropy. The parameter a_{ij} is mathematically the same as the deviatoric back-stress tensor. It incorporates the effect of inherent anisotropy on strength in a limited manner. Sands can be considered as a transversely isotropic material. Isotropy is assumed along the horizontal bedding plane. In the cases of bi-directional transverse shears, failure criteria should be identical for $\pm\tau_{zx}, \pm\tau_{yz}$, where z is normal to the bedding plane; furthermore, as $\sqrt{a_{ij}a_{ij}/2}$ is considerably smaller than η_{max}, a_{ij} can be neglected which enables significant simplification in the formulation without any appreciable error in the assumed load path.

Plastic potential. The deviatoric and hydrostatic components of the plastic potential are shown separately in Eq. 4. In conventional plasticity theory the plastic potential is a function of only stress invariants. This implies that the principal axes of stress and plastic strain increments coincide. A limitation of such a conventional plastic potential function is that it does not predict plastic strain increment for rotation of principal stresses which is often seen in sands. The flow rule for the deviatoric component was postulated in [5] from a series of experiments on Toyoura sand. The image point, X_{ij} depends on the direction of stress increment, l_{ij}; thus, by definition the model is hypoplastic and incrementally non-linear [4]. It may be noted that the scalar $\beta \geq 0$ can be solved by setting $F(X_{ij}) = 0$.

$$\partial g/\partial \sigma_{ij} = n_{ij}/\sqrt{2} + (\mu - c\eta)/3\,\delta_{ij} \tag{4}$$

where, $n_{ij} = \partial F/\partial r_{ij}$ at $r_{ij} = X_{ij}$; $n_{ij}n_{ij} = 1$; $X_{ij} = r_{ij} + \beta l_{ij}$; $l_{ij} = dr_{ij}/(r_{kl}r_{kl})^{1/2}$; and

$$c = r_{ij}d\varepsilon^p_{ij}/(r_{kl}r_{kl})^{1/2}\left(d\varepsilon^p_{mn}d\varepsilon^p_{mn}\right)^{1/2} \tag{5}$$

Stress-dilatancy relation. The hydrostatic component of the plastic potential function is the so-called stress-dilatancy relation. It has been conclusively shown in [3] that energy dissipation from plastic shear strain increment depends on the angle between the stress ratio and the plastic shear strain rate tensors. If the angle becomes small ($c \to 1$), then more energy dissipation will occur through shear deformation and less through volumetric deformation, and thus, dilatancy reduces with a decrease in angle (or with an increased value of c) and vice-versa. Any plasticity formulation in tri-axial stress space, which is also the principal stress space, does not allow for rotation of principal stresses; consequently, c implicitly becomes 1. The dilatancy coefficient μ is obtained from Eq. 6 [1].

$$\mu = \mu_0 + (2/\pi)(M - \mu_0)\tan^{-1}(\varepsilon^p/s_c) \tag{6}$$

Yield function and loading potential. The yield function is defined by Eq. 7. The loading potential is also divided in two components, deviatoric and hydrostatic. The yield surface is assumed to be infinitesimal because soil behaves non-linearly even at low strains.

$$f(\sigma_{ij}, \alpha_{ij}) = \sqrt{(s_{ij} - \alpha_{ij}p)(s_{ij} - \alpha_{ij}p)/2} - \eta p = 0 \quad (7)$$

An associated flow rule is assumed for the deviatoric component, while the hydrostatic component is derived from Eq. 7. The expression of the loading potential can be written as in Eq. 8.

$$\partial f/\partial \sigma_{ij} = n_{ij}/\sqrt{2} - c\eta/3\,\delta_{ij} \quad (8)$$

Plastic modulus. The stress increment in the sense of hypoelasticity can be considered to comprise two independent mechanisms, as shown in Eq. 9, by the terms dr_{ij} and dp, respectively [6]. It is assumed that only elastic strain increments will occur from the second mechanism. Hence, the model only considers the shear mechanism as depicted by the first term of dr_{ij} at a constant pressure.

$$d\sigma_{ij} = p dr_{ij} + (\sigma_{ij}/p) dp \quad (9)$$

Consequently, in the derivation of the plastic modulus as shown in Eq. 10, pressure is assumed as constant. The closed-form expression of $H_p$is available in [1].

$$H_p = \partial q/\partial \varepsilon^p = p\,\partial \eta/\partial \varepsilon^p;\ \eta = (G_N \varepsilon^p \eta_{max})/(G_N \varepsilon^p + \eta_{max}) \quad (10)$$

Plastic strain. Finally, expression of plastic strain can be derived by substituting Eq. 9,10 in Eq. 2. The closed form expression of λ is given in Eq. 11, which can be derived by noting that as $d\sigma_{ij} = p dr_{ij}$, $\partial f/\partial \sigma_{ij} d\sigma_{ij} = (p/\sqrt{2})\, n_{ij} dr_{ij}$.

$$\lambda = \left(2G d\varepsilon_{ij} n_{ij} - Kc\eta d\epsilon_{kk}\right)/\left[\sqrt{2}\{H_p + G - Kc\eta(\mu - c\eta)\}\right] \quad (11)$$

Hardening rule. Because the yield surface is vanishingly small, it will trivially satisfy the consistency at any point; in fact, for such case, there is no need to satisfy the consistency condition to derive the plastic modulus [4]. Instead, multiple nested loading surfaces having function of the form of Eq. 7 are used to describe plastic modulus at different stress states. The mixed evolution rule will require solution of two unknowns, α_{ij} and η, for which two independent equations are needed. One of the two equations is the consistency condition of loading surfaces, and the second equation can be framed from the condition that states that loading surfaces should be tangential. There is no concept of unloading as the yield surface is only a point and the mathematical reason is the hypoplasticity nature of the model; however, reloading condition for nth loading surface is given by Eq. 12.

$$\partial l^n/\partial r_{ij} dr_{ij} < 0\ ; \quad l^n(r_{ij}, \alpha_{ij}^n) = \sqrt{(r_{ij} - \alpha_{ij}^n)(r_{ij} - \alpha_{ij}^n)/2} - \eta^n = 0 \quad (12)$$

The plasticity formulation and hardening rules are illustrated in Fig. 1. As illustrated in Fig. 1b, the center of (n+1)th loading surface can be determined from the properties of nth loading surface using a recurrence relation, given in Eq. 13.

$$\alpha_{ij}^{n+1} = \alpha_{ij}^n + \beta^{n+1} p_{ij}^n;\ \ p_{ij}^n = (t_{ij}^n - \alpha_{ij}^n)/\sqrt{(t_{kl}^n - \alpha_{kl}^n)(t_{kl}^n - \alpha_{kl}^n)} \quad (13)$$

The scalar β^{n+1} can be solved by substituting Eq. 13 in Eq. 12 i.e. $l^{n+1}(r_{ij}, \alpha_{ij}^{n+1}) = l^{n+1}(t_{ij}^n, \alpha_{ij}^{n+1}) = 0$. The closed-form expression of β^{n+1} is given in Eq. 14.

$$\beta^{n+1} = \{t_{ij}^n(t_{ij}^n - \alpha_{ij}^n) + r_{ij}(\alpha_{ij}^n - r_{ij}) + \alpha_{ij}^n(r_{ij} - t_{ij}^n)\}/\{2p_{kl}(t_{kl}^n - r_{kl})\} \quad (14)$$

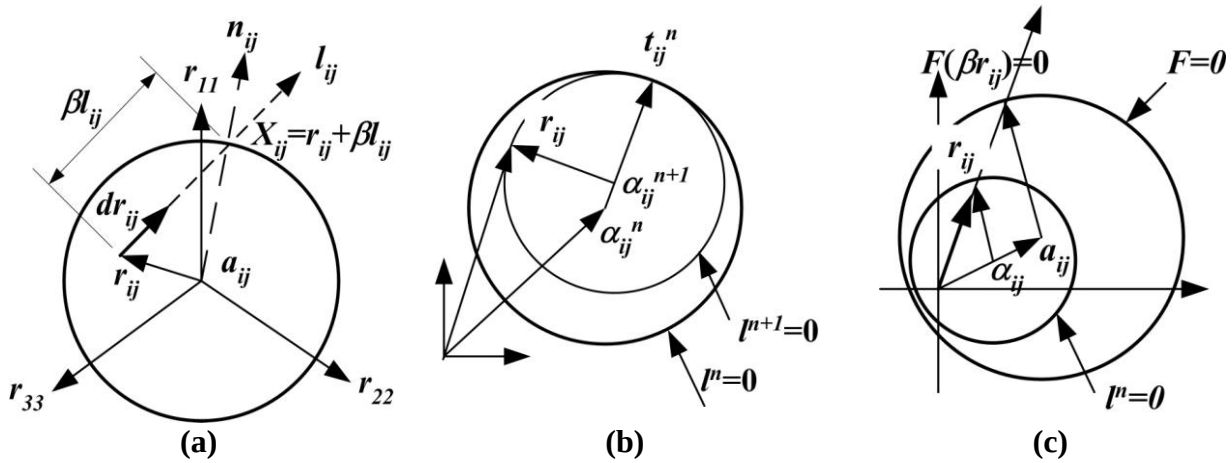

Figure 1 Geometrical interpretation of the model; (a) location of the conjugate point, X_{ij}, plastic shear strain increment direction, n_{ij} and stress increment direction, l_{ij}; (b) hardening rule with respect to general loading surfaces; (c) hardening rule of the virgin or the first loading surface, n=1.

In case of anisotropic failure surface, following hardening rule is proposed for n=1 loading surface based on Mroz's approach of homogeneous surfaces (see Fig 1c).

$$r_{ij} - \alpha_{ij}^{n} = \sqrt{r_{kl} r_{kl} / Y_{kl} Y_{kl}} \left(Y_{ij} - a_{ij}\right); \quad F\left(Y_{ij} = \beta r_{ij}\right) = 0 \tag{15}$$

Stress integration. Implicit stress integration has been adopted as per Eq. 16. As the elastic region is absent, the yield surface is a point that trivially satisfies the consistency condition, and the hardening rules are defined in terms of stress ratio, only the parameters of l_{ij} and c can be updated iteratively in each step (c^{t+dt} is obtained as the double contraction of unit tensors along r_{ij}^{t} and $d\varepsilon_{ij}^{p,t+dt}$).

$$\sigma_{ij}^{t+dt} = \sigma_{ij}^{t} + \chi\left(\sigma_{ij}^{t}, H_{p}^{t}, \mu^{t}, \eta^{t}, l_{ij}^{t+dt}, c^{t+dt}\right) d\epsilon_{ij}^{e} \tag{16}$$

State parameter. The constitutive parameters of η_{max} and G_N can be calibrated as linear functions of the state index defined in [2], which is a measure of relative state of a specimen with respect to the critical state line (either the steady state or quasi steady state) in void ratio versus pressure space; thereby, unifying the properties for different relative densities in a single expression.

Model parameters

The model parameters are adopted from [1]. Because the present model is only a mathematical extension of the two-dimensional model, it is sufficient to only verify the implementation of the three-dimensional form. If tensors are reduced to that of a plane-stress form, then the explicit formulas given in [1] can be retrieved. For the purpose of verification, the same models parameters as that of the plane-strain model for Toyoura sand [1] are used.

Verification

Undrained simulations. Undrained strain controlled cyclic simulations are carried out for Toyoura sand with void ratios of 0.75 and 0.8 (relative densities of ~60% and ~50% respectively). The simulations are conducted for the torsional stress path (b = 0.5) consisting of identical bi-directional shear strain cycles of ϵ_{zx} and ϵ_{yz} under uniform stress cycles of constant amplitude of η = 0.2. The results are shown in Fig. 2 for the respective void ratios with an initial effective pressure p = 100kPa. It can be seen that the gradual loss of the effective pressure leading to cyclic mobility can be satisfactorily captured by the model. It is notionally considered that the process of liquefaction starts when the effective pressure is reduced to half. In case of the sand with void ratio of 0.75, the

number of cycles to liquefaction is nearly 4, while that of the sand with void ratio of 0.8 is almost 1.5. This difference is due to the different values of the state index values for the respective sands.

Drained simulations. Drained (p constant) simulations are carried out for void ratio of 0.75 under independent bi-directional random stress cycles in torsional stress path comprising τ_{zx} and τ_{yz} The orthogonal stress history is synthesized from the ground acceleration recorded at Urayasu (CHB008 of K-NET array [7]) during the M_w9 11 March 2011 Tohoku earthquake. This is a long duration earthquakes (of duration approximately 300 sec) consisting of many irregular stress cycles, most suitable for rigorously verifying the implementation of the hardening rule. The peak ground acceleration corresponds to the pre-determined stress ratio (η_{peak}) which defines the radius of the largest loading surface.

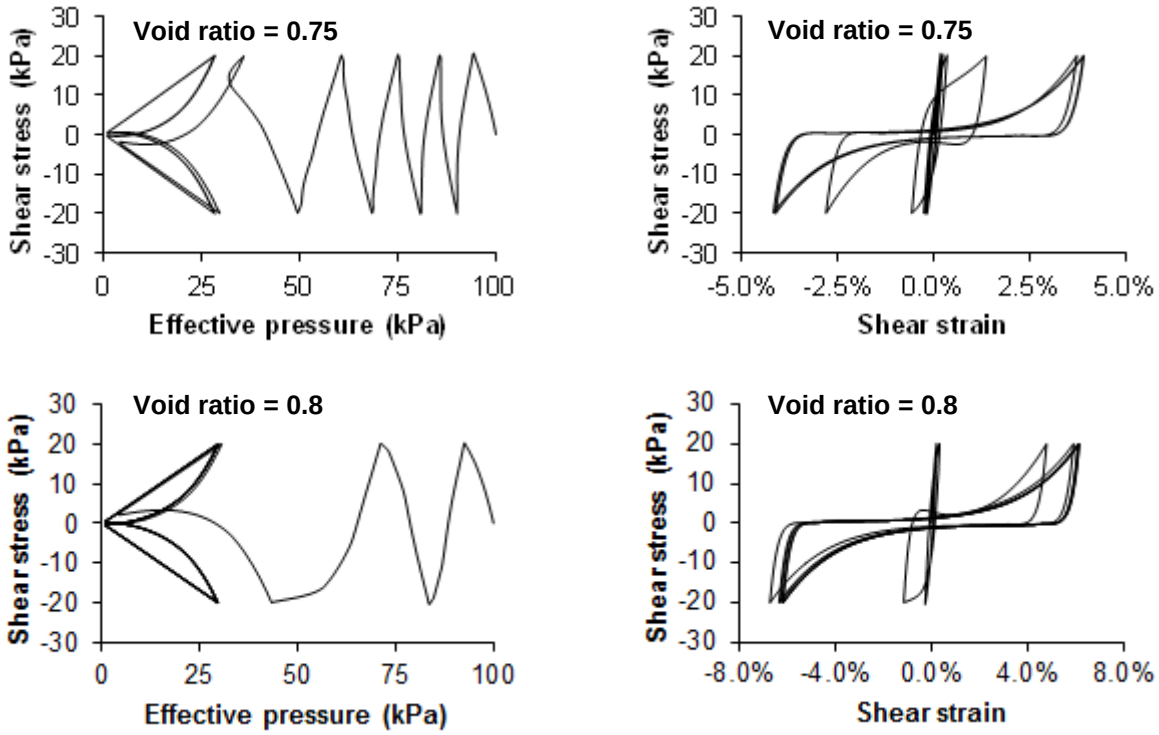

Figure 2 Strain controlled simulation of Toyoura sand for void ratios of 0.75 and 0.8 under identical bi-directional shear strain cycles of ϵ_{zx} and ϵ_{yz} conforming to the torsional stress path (b=0.5) with η=0.2 and p=100kPa using the model parameters available in [1]; the shear strain is defined the same way as the generalized plastic shear strain, but with the total strain tensor

The effective pressure is kept constant at 100kPa and $\eta_{peak}$is varied as 0.2, 0.4 and 0.6 to illustrate three different levels of inelastic actions, low, moderate and high, respectively. The orthogonal converted stress histories are shown for η_{peak}= 0.6 in Fig 3a; τ_{zx} is the principal direction because both positive and negative peaks are greater than those of τ_{yz}. Fig 3b shows that the polarization of the vertically upward propagating shear wave is complex; the corresponding hysteresis loops are shown in Fig 3c. The hysteresis loops are stable and closed, producing positive area indicating energy dissipation. It can be observed that energy dissipation under $\tau_{zx} - \epsilon_{zx}$ hysteresis curve is greater than that of the $\tau_{yz} - \epsilon_{yz}$ (60%: 40%), as the former is the principal direction; this is also reflected in the respective maximum strain limits. The time series plots of the strains for η_{peak}= 0.6 are shown in Fig 3d for the time interval 100-160 sec when the response is most significant. The peak values are highlighted with open circles. Fig 3d also shows the build-up of volumetric strain due to dilatancy. It can be noted that the higher the stress level, the greater is the dilatancy; q_{max} = 60, 40 and 30kPa correspond respectively to η_{peak}=0.2, 0.4 and 0.6 at the constant p =100kPa. Most of the volumetric strain is accumulated by 150 sec, which is also indicative of the significant duration of the ground motion. The significant duration of the principal direction based on 90% of cumulative Arias intensity is also around 150 sec. Hence, the hardening rule is capturing the cumulative effect satisfactorily.

Summary and conclusion

The present work extends an existing plane-strain constitutive model to three dimensions within the classical plasticity framework. While the plane-strain model provides a physical interpretation of the constitutive behaviour, the present approach provides an elegant mathematical interpretation for generalized stress conditions. An anisotropic failure surface with an additional mixed hardening rule is proposed to combine the effects of inherent anisotropy and the *b* value. Strain-controlled simulations for the bi-directional simple shear are satisfactorily capturing the phenomenon of cyclic mobility. The implementation of the hardening rule is also verified under bi-directional, complex stress histories for which the model is intended for use.

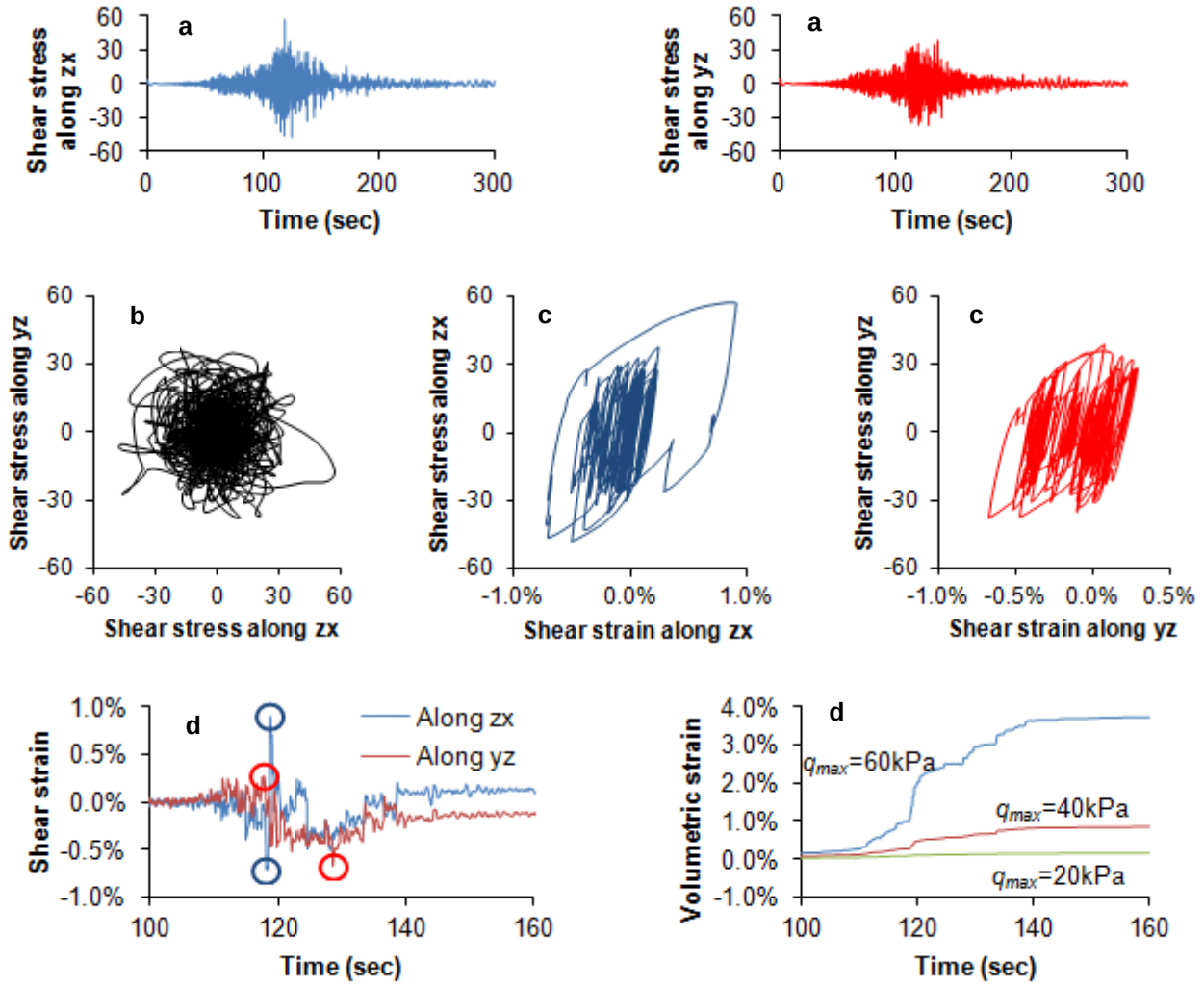

Figure 3 Stress controlled simulation of Toyoura sand with void ratio of 0.75 and p=100kPa using the model parameters of [1] (stresses are in kPa); (a) time series plots of orthogonal stress inputs for $\eta_{peak} = 0.6$ synthesized from ground acceleration recorded at Urayasu (CHB008 of K-NET array [7]) during the Mw9 11 March 2011 Tohoku earthquake; (b) corresponding plot of τ_{yz} versus τ_{zx} indicating a random polarisation; (c) corresponding hysteresis plots along the respective directions as indicated; (d) time series plots of shear strain and volumetric strain due to dilatancy

References

[1] M. Cubrinovski, K. Ishihara, State concept and modified elastoplasticity for sand modeling, Soils and Foundations 38(4) (1998) 213-225

[2] M. Cubrinovski, K. Ishihara, Modelling of sand behaviour based on state concept, Soils and Foundations 38(3) (1998) 115-127

[3] M. Gutierrez, K. Ishihara, Flow theory for sand during rotation of principal stress direction, 40(2), Soils and Foundations (2000) 49-59

[4] Y. F. Dafalias, Bounding surface plasticity. I: Mathematical foundation and hypoplasticity, ASCE Journal of Engineering Mechanics 112(9) (1986) 966-987

[5] M. Gutierrez, K. Ishihara, I. Towhata, Flow theory for sand during rotation of principal stress direction, 31(4), Soils and Foundations (1991) 121-132

[6] Z. L. Wang, Y. F. Dafalias, C. K. Shen, Bounding surface hypoplasticity model for sand, ASCE Journal of Engineering Mechanics 116(5) (1990) 983-1001

[7] Information on http://www.kyoshin.bosai.go.jp

Appendix: List of symbols

$\epsilon_{ij}, \epsilon_{ij}^{e}, \epsilon_{ij}^{p}$: Total, elastic and plastic strain tensors, respectively
q : Generalized shear stress
s_{ij} : Deviatoric stress tensor
η : Shear stress ratio
$p = \sigma_{ii}/3$: Effective pressure
$r_{ij} = s_{ij}/p$: Deviatoric stress ratio tensor
λ : Generalized plastic strain increment
$\varepsilon_{ij}, \varepsilon_{ij}^{e}, \varepsilon_{ij}^{p}$: Deviatoric total, elastic and plastic strain tensors, respectively
ε^{p} : Generalized accumulated plastic strain
g : Plastic potential function
σ_{ij} : Stress tensor
H_p : Plastic modulus
f : Yield function
E_{ijkl} : Rank four elastic constitutive tensor
F : Bounding or failure surface
a_{ij} : Origin of the failure (bounding) surface
η_{max} : Maximum value of shear stress ratio
$J_2 = s_{ij}s_{ij}/2$: Second deviatoric stress invariant
$J_3 = s_{ij}s_{jk}s_{ki}/3$: Third deviatoric stress invariant
$b = (\sigma_2 - \sigma_3)/(\sigma_1 - \sigma_3)$: Lode's parameter, $\sigma_1 > \sigma_2 > \sigma_3$ are principal stresses
μ : Dilatancy coefficient
c : Non-coaxiality parameter
δ_{ij} : Kronecker's delta
n_{ij} : Unit tensor defining the direction of plastic strain increment
X_{ij}, Y_{ij} : Conjugate or image points
β, β^{n+1} : Positive scalars, defining magnitude of a tensor
l_{ij} : Unit tensor defining the direction of stress ratio increment
$\mu_{0;}M$: Dilatancy coefficient at small and large strains respectively
s_c : Parameter controlling rate of dilatancy with accumulated plastic strain
α_{ij} : Deviatoric back-stress tensor of yield and loading surfaces
G_N : Initial tangent (plastic modulus) of the backbone curve see Eq. 10
G : Elastic shear modulus
K : Elastic bulk modulus
l^n : Loading surface, superscript denotes the number of surface
p_{ij}^{n} : Unit tensor defining radial direction of a loading surface
t_{ij}^{n} : Deviatoric stress ratio tensor at reversal point from n^{th} loading surface.